Available online at website: https://journal.bcrec.id/index.php/bcrec

Bulletin of Chemical Reaction Engineering & Catalysis, 20 (2) 2025, 371-380

Original Research Article

Low Temperature Synthesis of Biodiesel via Heterogeneous Potassium-Alumina Catalyst

Aghietyas Choirun Az Zahra[1,3], Geraldi Cengko[3], Azra Hijran[3], Jenny Rizkiana[1,2,3*]

[1]Department of Bioenergy Engineering and Chemurgy, Institut Teknologi Bandung, Sumedang, 45363, Indonesia
[2]Center for Catalysis and Reaction Engineering, Institut Teknologi Bandung, Bandung, 40132, Indonesia
[3]Department of Chemical Engineering, Institut Teknologi Bandung, Bandung, 40132, Indonesia

Received: 7th February 2025; Revised: 2nd May 2025; Accepted: 2nd May 2025
Available online: 4th May 2025; Published regularly: August 2025

Abstract

Indonesia, one of the world's largest producers of crude palm oil (CPO), is aiming to achieve a renewable energy mix target of 23% by 2025 through the implementation of a B35 policy, blending diesel with fatty acid methyl ester (FAME) derived from CPO transesterification. Traditionally, homogeneous catalysts are used in this process, but their sensitivity to free fatty acids reduces biodiesel yield. Therefore, heterogeneous catalysts are being developed to overcome this issue, contributing to sustainable biodiesel production. However, certain heterogeneous catalysts require high temperature, more methanol, longer reaction times, necessitating the exploration of more optimal catalyst options. This study introduces an approach by exploring the use of heterogeneous $K_2O/\gamma\text{-}Al_2O_3$ catalysts in biodiesel production from RBDPO under low-temperature conditions (40 °C), a significant reduction from the commonly operated temperature of near the boiling point of methanol at 60 °C. Utilizing KI and KNO_3 as precursors, the effect on different catalyst precursor, temperatures and reaction time were examined. It was found that temperature has the highest effect on conversion. The transesterification process yielded biodiesel with FAME levels ranging from 95.84% to 98.17%, meeting the Indonesian National Standard (SNI 7182:2015) for biodiesel quality. The findings indicate that both KI and KNO_3 precursors result in highly active $K_2O/\gamma\text{-}Al_2O_3$ catalysts, achieving high conversion at 40 °C within a 1-hour reaction time, thus demonstrating their effectiveness in low-temperature biodiesel synthesis. This low-temperature process has the potential to significantly reduce energy consumption in industrial biodiesel production.

Keywords: Biodiesel; FAME yield; heterogeneous catalyst; $K_2O/\gamma\text{-}Al_2O_3$ catalyst; low temperature synthesis

How to Cite: Az Zahra, A. C., Cengko, G., Hijran, A., Rizkiana, J. (2025). Low Temperature Synthesis of Biodiesel via Heterogeneous Potassium-Alumina Catalyst. *Bulletin of Chemical Reaction Engineering & Catalysis*, 20 (2), 371-380. (doi: 10.9767/bcrec.20349)

Permalink/DOI: https://doi.org/10.9767/bcrec.20349

1. Introduction

Biodiesel is an environmentally friendly, renewable, and sustainable fuel that has the potential to replace petroleum-based diesel fuel [1–3]. Currently, Indonesia is a leading country in the biodiesel utilization with its B35 policy, which mandates a 65:35 blend of petroleum diesel and fatty acid methyl ester (FAME) derived from crude palm oil (CPO) in the domestic market [4]. In 2024, Indonesia produced nearly 14 million kiloliters of biodiesel, with 99% consumed domestically, as reported by Indonesian Biofuel Producers Association (APROBI). As one of the world's largest fossil fuel consumers, Indonesia stands to enhance its energy security through a robust domestic biodiesel industry.

Biodiesel, or fatty acid methyl ester (FAME), is a renewable liquid fuel derived from sources such as vegetable oil, with crude palm oil (CPO) being a primary feedstock in Indonesia. Refined Bleached Deodorized Palm Oil (RBDPO) undergoes transesterification to produce biodiesel [5]. Transesterification, a key process in biodiesel production, involves converting triglycerides into

* Corresponding Author.
Email: rizkiana@itb.ac.id (J. Rizkiana)

diglycerides and monoglycerides, which react with methanol to yield FAME and crude glycerol [6]. Research efforts are focused on producing biodiesel with higher FAME content, which could lead to more efficient production processes.

The conversion of vegetable oils and animal fats to biodiesel requires catalysts to facilitate the transesterification reaction [7]. Conventional transesterification typically uses basic homogeneous catalysts (e.g., KOH or NaOH) due to their high catalytic activity and short reaction times [8]. While these conventional homogeneous base catalysts are favored, they have drawbacks including sensitivity to free fatty acids and challenges in recovery and reuse [9,10]. Therefore, exploring alternative catalysts, such as heterogeneous catalysts, is essential. Heterogeneous catalysts offer advantages such as easy recovery, reusability, simpler purification, and lower costs, making them suitable for continuous biodiesel production in fixed-bed reactors on an industrial scale [9,11,12]. These catalysts will enable efficient and economical biodiesel production.

For industrialization purposes, heterogeneous base catalysts should possess the following characteristics: (1) safety, with no volatility, corrosivity, or toxicity; (2) low cost, being commercially available or easily prepared at a lower price; (3) chemical stability and high reusability; and (4) high activity at ambient temperature [13]. In FAME synthesis via transesterification, temperature is a crucial parameter. This conversion process is limited by the boiling point of methanol (65 °C) necessitating low-temperature conditions [14]. Hence, the research around FAME synthesis is mostly conducted at a temperature near the boiling point of methanol, of 50-65 °C [15–18]. Moreover, higher temperature leads to a higher reaction rate, which increases the favorability of biodiesel formation [18,19]. A much lower temperatures (35-50 °C) have been associated with unsatisfactory conversion rates of triglycerides [14–16].

To address these challenges, this study evaluates the effectiveness of $K_2O/\gamma\text{-}Al_2O_3$ catalysts in the production of biodiesel from RBDPO, conducted in a lower temperature of 40°C and higher temperature commonly operated at 60 °C. This $K_2O/\gamma\text{-}Al_2O_3$ catalyst is a solid base catalyst, with $\gamma\text{-}Al_2O_3$ chosen as the support due to its high mechanical strength, large surface area, and cost-effectiveness [20]. Meanwhile, potassium has been proven effective in homogeneous catalyst for biodiesel production. This study investigates the impact of different precursor: KI and KNO_3, reaction time, and temperatures on catalyst performance to identify the optimal configuration. The objectives include determining the FAME content in biodiesel produced with the $K_2O/\gamma\text{-}Al_2O_3$ catalyst and assessing the relationship and importance of reaction temperature, reaction time, and catalyst precursor on the FAME content in the biodiesel generated using the $K_2O/\gamma\text{-}Al_2O_3$ catalyst.

2. Materials and Method

2.1 Catalyst Synthesis and Transesterification Process

The $K_2O/\gamma\text{-}Al_2O_3$ catalyst was synthesized through the wet impregnation method. Initially, a specific quantity of $\gamma\text{-}Al_2O_3$ was submerged and agitated in an aqueous solution containing either KI or KNO_3 for a duration of 2 hours. These potassium precursor was chosen due to both KI and KNO_3 having a high basic strength that leads to a high conversion activity on biodiesel synthesis compared to other potassium compounds such KCl, KBr, and K_2CO_3 [21,22]. After the wet impregnation, the surplus water was eliminated by subjecting the mixture to drying in an oven at 100 °C for 24 hours. Following this, the catalyst underwent calcination at 700 °C for 3 hours, resulting in the formation of the dried $K_2O/\gamma\text{-}Al_2O_3$ catalyst. Catalyst characterization includes X-Ray Diffraction (XRD), Brunauer-Emmett-Teller (BET), and Temperature Programmed Desorption (TPD).

For the transesterification process, a 1000 mL three-neck flask equipped with a reflux condenser and magnetic stirrer was used. RBDPO was heated to the desired temperature, then mixed with methanol and $K_2O/\gamma\text{-}Al_2O_3$ catalyst. The reaction was conducted at 600 - 750 rpm for 1-3 hours at a pre-determined temperature and holding time variation. After completion, the catalyst was separated filtration, and the biodiesel was isolated from the remaining methanol and glycerol using a separatory funnel for 24 hours. The biodiesel was washed three times with water and dried at 80 °C for 1 hour. Acid value, total glycerol content, and saponification value were analyzed to determine the FAME content and yield, with experiments replicated for all design variations.

The FAME content analysis involved acid value analysis, total glycerol content analysis, and saponification value analysis, in accordance with SNI No. 7182 Year 2015. The acid value is determined by titrating the biodiesel sample with 0.1 N KOH, then calculated using Equation (1). The total glycerol content was determined by saponifying the sample with alcoholic KOH and glacial acetic acid, followed by titration with sodium thiosulfate. Saponification value was measured by boiling biodiesel with alcoholic KOH, followed by titration using 0.5 N HCl with phenolphthalein as the indicator. The FAME content was calculated using the Equation (2):

$$A_a = \frac{56.1 \times V \times N}{m} \quad (1)$$

$$\%m_{FAME} = \frac{100 \times (A_s - A_a - 18.29 \times \%m_{glycerol,total})}{A_s} \quad (2)$$

where A_a is the acidic value of the sample (mg KOH/g biodiesel), V is the titration volume of KOH 0.1 N, N is the exact normality of the KOH solution, and m is the weight of the sample (g). Whereas the saponification value of the biodiesel sample (mg KOH/g biodiesel), A_a is the acidic value of the biodiesel sample (mg KOH/g biodiesel), and $\%m_{glycerol,total}$ is the total glycerol content within the biodiesel sample.

2.2 Design of Experiments

The experimental design in this research was conducted by using two level full factorial design with three factors: reaction temperature, reaction time, and catalyst precursor. The center point was replicated three times. The experimental design is presented in Table 1. After conducting the experiment with all determined variations, experimental analysis was performed using Minitab 23 to determine the statistical significance of each factor and its effects on catalyst performance. The mathematical model representing the catalyst performance is given by the Equation (3):

$$Y = \beta_o + \beta_1 X_1 + \beta_2 X_2 + \beta_3 X_3 + \beta_{12} X_1 X_2 + \beta_{13} X_1 X_3 + \beta_{23} X_2 X_3 + \beta_{123} X_1 X_2 X_3 \quad (3)$$

whereas, X_1 is reaction time, X_2 is reaction temperature, X_3 is catalyst precursor, and β is the coefficient of regression results on each factor.

3. Results and Discussion

3.1 Synthesis and Characterization of Catalysts

The characterization carried out for the K_2O/γ-Al_2O_3 catalyst with KI precursor (denoted as KI/γ-Al_2O_3) and KNO_3 precursor (denoted as KNO_3/γ-Al_2O_3) includes X-Ray Diffraction (XRD) and Nitrogen Adsorption Isotherms. The characterization results are summarized in Figure 1 and Table 2. From the BET analysis in Table 2, KI and KNO_3 were successfully loaded into loaded onto the γ-Al_2O_3 support material, with 36% loading on KI/γ-Al_2O_3 and 35% loading on KNO_3/γ-Al_2O_3. The average pore size of the catalyst indicates that both catalysts fall into the mesoporous catalyst (2-50 mm). The BJH adsorption surface area is 120.979 m^2/g for KI/γ-Al_2O_3 and 85.534 m^2/g for KNO_3/γ-Al_2O_3, demonstrating that a substantial amount of surface area remains available for catalytic reactions. The approximately 35.445 m^2/g lower surface area for KNO_3/γ-Al_2O_3 can be attributed to the different properties and behaviors of the KI and KNO_3 precursors. The nature and size of the anions likely play a significant role. The larger iodide ions from KI form weaker interactions with alumina support, resulting in more dispersed potassium deposition and less pore blockage. In contrast, the highly polar nitrate ions from KNO_3 in aqueous solution form strong interactions and hydrogen bonds on the gamma alumina surface [23], leading to more uniform and extensive coverage, greater pore blockage, and a significant reduction in surface area. Additionally, the smaller nitrate ions can penetrate deeper into the alumina pores, blocking more internal surface

Table 1. Experimental design

Factor	Lower Threshold	Upper threshold
Time (hour)	1	3
Temperature (°C)	40	60
Precursor	KI	KNO_3

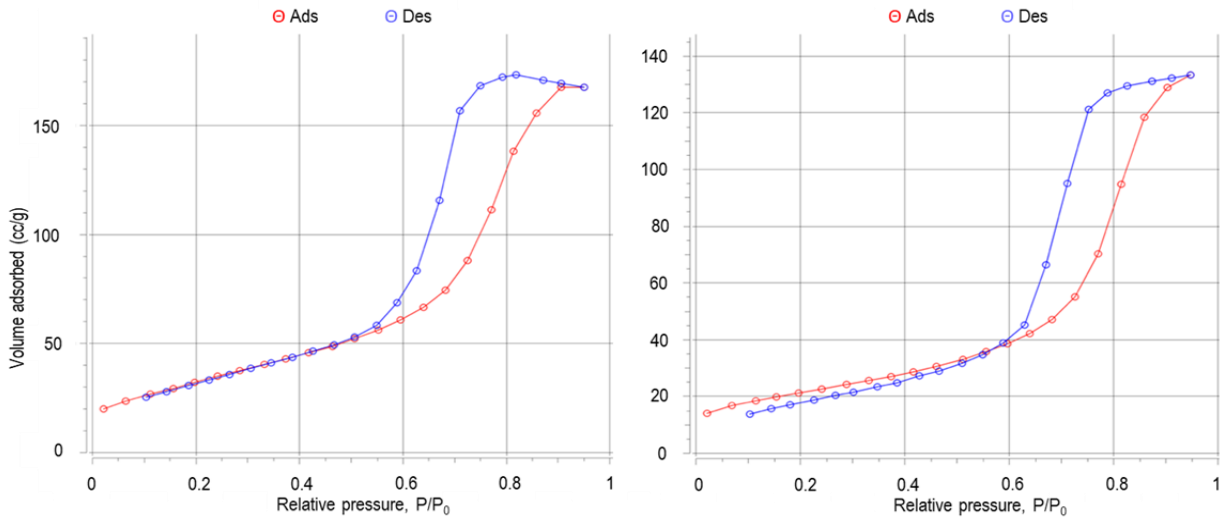

Figure 1. Nitrogen adsorption isotherm result of catalyst A (left) and B (right)

area, whereas the larger iodide ions interact more at the surface level, preserving more internal porosity. The pore volume is measured at 0.254 cm^3/g for KI/γ-Al_2O_3 and 0.202 cm^3/g for KNO_3/γ-Al_2O_3, which indicates KI/γ-Al_2O_3 has a more significant total volume of pores within the catalyst. The pore radius of both catalysts aligns closely with the average pore size, confirming a consistent and uniform pore structure.

Figure 1 shows that the catalyst exhibits a Type IV isotherm, typical of mesoporous materials. The hysteresis loop between the adsorption (red curve) and desorption (blue curve) branches indicates capillary condensation within the mesopores. The loop closure at higher relative pressures around 0.9 suggests the presence of larger mesopores or possible interparticle voids, while the steep rise and fall in the adsorption-desorption branches suggest cylindrical or ink-bottle shaped pores. This nitrogen adsorption-desorption isotherm confirms that both KI and KNO_3 loading in the γ-Al_2O_3 support material results in a well-defined mesoporous structure.

The X-ray diffraction analysis is presented in Figure 2. The X-ray diffraction (XRD) analysis of KI/γ-Al_2O_3 shows distinct peaks at 31°, 36°, 45°, and 66°. These peaks align with gamma alumina's characteristic peaks at 37°, 45°, and 66° (JCPDS 10−173), thus confirming the presence of alumina support. The peaks at 31°, 39°, and 62° suggests the presence of potassium oxide (JCPDS 47−1701), indicating successful KI and KNO_3 impregnation and calcination into K_2O [21]. Figure 2 shows a prominent K_2O peak suggesting a high KI or KNO_3 loading ratio. Both catalysts show phases of gamma alumina, but the potassium compound peaks differ slightly, reflecting the varying interactions of KNO_3 and KI with the gamma alumina support. Nevertheless, the overall XRD peaks shown in both catalysts confirm the amorphous structure.

The thermal decomposition behaviors of KI and KNO_3 also differ. KI decomposes relatively easily, releasing iodine and forming potassium oxide without major structural changes to the alumina, thereby preserving more surface area. However, KI remnants were found at 21° and 25°, suggesting excessive loading in the catalyst [24]. Conversely, KNO_3 decomposes with the release of gases such as NO_x and oxygen, which can induce increased pressure within the pores and local overheating. This may cause sintering and phase transformations in the alumina, resulting in larger potassium oxide clusters (agglomeration) that block more pores and substantially reduce the surface area. This was evidenced by a peak found around 27°, which could be assigned to the $K_2[Al(NO_3)_5]$ intermediate [25].

3.2 Low Temperature FAME Synthesis with K_2O/γ-Al_2O_3 Catalyst

3.2.1 Optimization of FAME synthesis parameters

The results obtained of acid number, saponification value, total glycerol levels, and FAME content from every variation of the

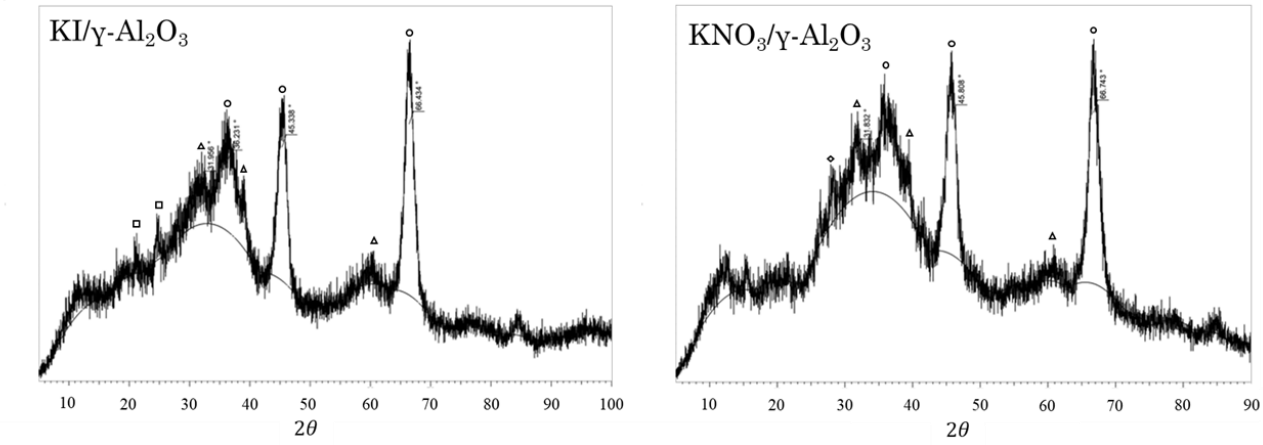

Figure 2. XRD of KI/γ-Al_2O_3 catalyst (left) and KNO_3/γ-Al_2O_3 (right) (□ KI, △ K_2O, ○ Al_2O_3, ◇ $K_2[Al(NO_3)_5]$)

Table 2. Pore size and volume of Catalyst A and B

Catalyst	Metal content	Avg. Pore Size (nm)	BJH Adsorption		
			Surface Area (m^2/g)	Pore Volume (cm^3/g)	Pore Radius Dv (nm)
KI/γ-Al_2O_3	0.36	4.305	120.979	0.254	4.259
KNO_3/γ-Al_2O_3	0.35	5.41	85.534	0.36	5.41

experiment are shown in Table 2. The results are then analyzed using full factorial design analysis using Minitab 23. The mathematical model of experimental design can be represented by the Equation (4). The diagnostic curves and the significance curve of the analysis are shown in Figure 3 and Figure 4:

$$Y(\%) = 99.64 - 2.315\,Time - 0.0607\,Temperature + 0.0490\,Time \times Temperature + 0.037\,C_tP_t \quad (4)$$

where, C_tP_t is the binary variable that represents the center point variation (0 for non-center point variation and 1 for center point variation).

Based on the Pareto chart (Figure 4) and residual plots (Figure 3), a detailed analysis of the full factorial design model's validity was conducted using ANOVA. The residual distribution curve and histogram indicate that the residuals are normally distributed. The correlation curve between the residuals and the fitted values (Figure 3.5b) shows that all residuals fall within the upper and lower limits, confirming the assumption of homoscedasticity. These analyses confirm that all ANOVA assumptions are met, validating the model. The Pareto chart in Figure 4 identifies significant variables affecting FAME levels: the interaction between time and temperature (BC), temperature alone (C), and time (B), all of which have standardized effects exceeding the critical value of 2.571. This indicates these factors significantly influence the FAME yield (p-value < 0.05). Consequently, both the interaction of time and temperature, as well as these individual factors, play crucial roles in determining the FAME content in biodiesel. The factorial plot representing the individual and interactional effects of each experimental factors are shown in Figure 5.

The main effects plot for yield in Figure 5 shows that the precursor type (KI or KNO_3) has relatively minimal impact to the yield, with mean yields remaining nearly constant regardless of the precursor used. In contrast, increasing the reaction time from 1 to 3 hours significantly affected the yield, indicating that longer reaction times allow for more reactant conversion. The most significant impact on yield is observed with reaction temperature, increasing the temperature from 40 °C to 60 °C results in a substantial increase, likely due to enhanced reaction rates

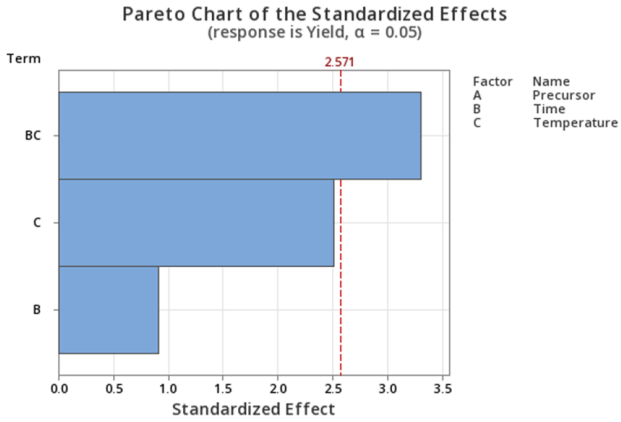

Figure 4. Statistical significance of each factor.

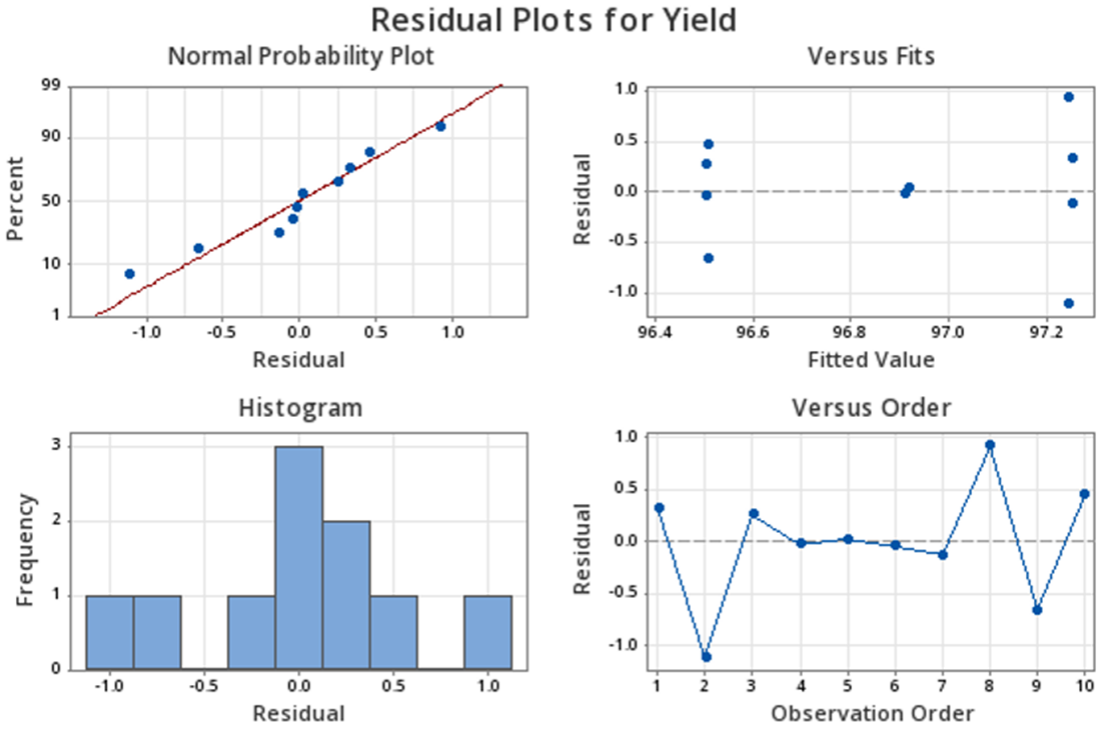

Figure 3. Diagnostic curves of the full factorial design analysis.

and efficiency. Thus, optimizing reaction temperature and time is crucial for maximizing yield, while the choice of precursor has minimal impact. This analysis highlights the importance of fine-tuning reaction conditions to enhance biodiesel production efficiency and yield. Overall, the biodiesel produced with the K_2O/γ-Al_2O_3 catalyst had FAME content ranging from 95.84% to 98.17%. Based on SNI standards of SNI 7182:2015, which dictates that the FAME content of biodiesel needs to be higher than 96.5%, all the biodiesel samples produced in this experiment were able to fulfil the standard except one.

On the physical properties of FAME, based on the results of viscosity measurements from each experimental variation, the kinematic viscosity of the samples ranged from 4.54 to 17.19 mm²/s, with an average of 10.72 mm²/s. This range indicates moderate variation in viscosity across different experimental conditions, with the average value still falling outside the SNI 7182:2015 viscosity range of 2.3-6.0 mm²/s. Only one experimental variation met the standard with a value of 4.54 mm²/s. A noticeable negative correlation exists between viscosity and FAME conversion; samples with higher viscosity tend to have lower conversion percentages. Residual glycerol from incomplete washing is a potential reason for the elevated viscosity values. Glycerol, a byproduct of the transesterification process, is highly viscous, and its incomplete removal can lead to higher overall viscosity in the final biodiesel product. To ensure that biodiesel viscosity meets the SNI 7182:2015 standards, optimizing the transesterification reaction to achieve higher FAME conversions is crucial. This involves thorough washing to remove residual glycerol and further increasing conversion efficiency.

3.2.2 Effect of precursor towards FAME yield

In this study, two different potassium precursors were used, KI and KNO_3. Although both are strong base precursors theoretically leading to high conversion to FAME, a previous study by Xie and Li on biodiesel synthesis from soybean oil reported that KI achieved a higher conversion rate compared to KNO_3, with 87.4% versus 67.4% [21]. The conversion results to FAME using RBDPO in this study are presented in Figure 6, which includes the lower and upper thresholds of the experimental design without the center point.

As seen in Figure 6, all the variations result in a high FAME yield of more than 95%, indicating that the catalyst has successfully

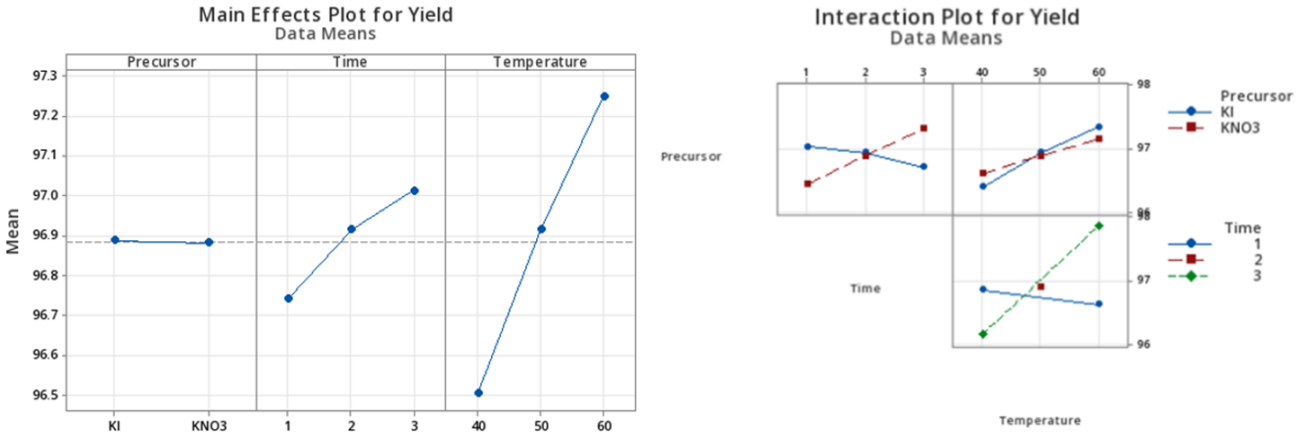

Figure 5. Main effects and interaction plot of experimental factors.

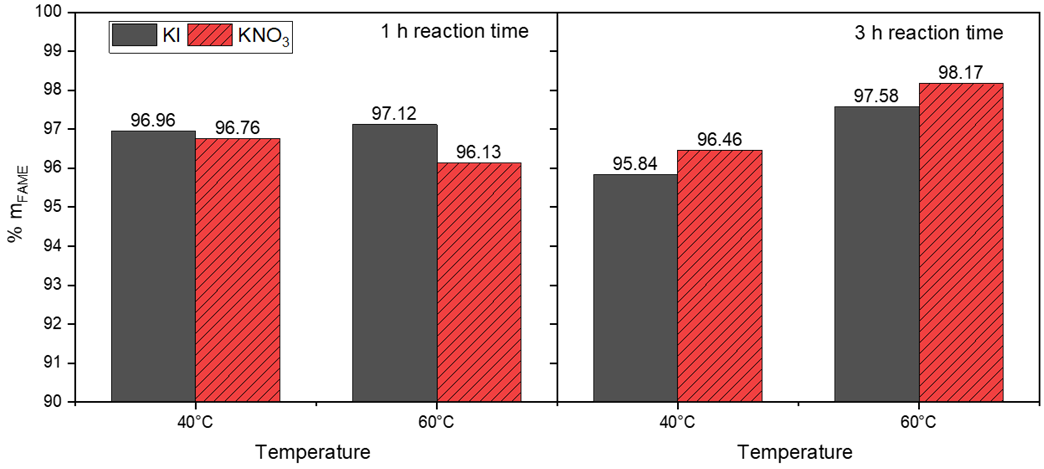

Figure 6. Effect of temperature on FAME yield.

catalyzed the transesterification of RBDPO to FAME. In 1 hour of reaction time, the KI precursor proves more effective in the transesterification process, leading to a slightly higher yield compared to the KNO_3 precursor. This is mainly due to the higher surface area of KI, allowing more substances to be adsorbed onto the catalyst surface. This result applies to both operating temperatures, 40 °C and 60 °C. However, with longer reaction times, the opposite occurs, with the KNO_3 precursor achieving a higher FAME conversion rate compared to the KI precursor. Over prolonged periods, KNO_3 has shown slightly better performance compared to KI. However, the difference in FAME yield between the precursors is only around 1% in each variation, suggesting that there might not be enough data to prove a significant difference. Based on the statistical analysis in the previous section, the effect of different precursors is almost negligible, indicating that both KI and KNO_3 can be used in FAME production with similar performance.

It is important to highlight that while using alkaline catalysts, either homogeneous or heterogeneous, in biodiesel production, there might be some poisoning occurring. Alkaline catalysts can undergo poisoning due to factors such as the presence of water, free fatty acids (FFA), and phospholipids [26,27]. However, further study and analysis are needed to conclude whether poisoning occurred in this study.

3.2.3 Effect of reaction time on FAME

The effect of reaction time on FAME yield is more significant than the effect of the potassium precursor, although it is still not the most critical parameter. Previous researchers have explained that longer reaction times generally lead to higher conversion to FAME [28,29]. In this study, the effect of reaction time on FAME yield was investigated by comparing two different durations: 1 hour and 3 hours. The results indicate that extending the reaction time generally leads to a slight improvement in FAME yield, as presented in Figure 6. For instance, using KI at 60 °C resulted in a conversion of 97.12%, which increased to 97.58% after extending the reaction time to 3 hours.

The increase in FAME yield with longer reaction time can be attributed to the more complete conversion of triglycerides to FAME. During the initial stages of the reaction, the catalyst facilitates the transesterification process, converting triglycerides into FAME and glycerol. As the reaction progresses, the remaining unreacted triglycerides continue to be converted, leading to a higher overall yield. This trend is consistent with previous studies, which have shown that longer reaction times can enhance conversion efficiency in biodiesel production.

However, the relatively small difference in yield (around 1%) after increasing the reaction time suggests that the reaction reaches near-completion within the first hour. This implies that the potassium-alumina catalyst used in this study is highly effective, achieving high conversion rates in a relatively short period. The marginal increase in yield with extended reaction time may not justify the additional energy and time costs in practical biodiesel production. This also indicates that the catalyst's performance is robust and not significantly influenced by these variables within the tested range.

3.2.4 Effect of temperature on FAME yield

Temperature significantly impacts reaction kinetics and FAME yield. This study highlights the performance of biodiesel production from RBDPO to FAME at lower temperatures assisted

Table 3. FAME content results of each variation.

Run	Precursor	Time (h)	Temperature (°C)	Total $\%m_{\text{glycerol}}$	$\%m_{\text{FAME}}$
1	KI	1	40	0.28	96.96
2	KI	3	40	0.32	95.84
3	KI	1	60	0.25	97.12
4	KI	3	60	0.24	97.58
5	KI	2	50	0.27	96.94
6	KNO_3	1	40	0.19	96.76
7	KNO_3	3	40	0.24	96.46
8	KNO_3	1	60	0.20	96.13
9	KNO_3	3	60	0.20	98.17
10	KNO_3	2	50	0.23	96.89

by a heterogeneous catalyst. Previous studies have mostly reported that biodiesel production is favorable at higher temperatures of 60 °C or above, as it leads to higher conversion rates [14–17]. Reviewing the kinetics of the transesterification reaction, the process of producing biodiesel is endothermic [19,27]. In an endothermic reaction, increasing the temperature favors product formation and increases the reaction rate. This is supported by previous research by Xiao *et al*. which indicated that the kinetics of the transesterification reaction of palm oil with methanol obey the Arrhenius law, where an increase in temperature leads to an increase in the kinetics constant [30].

As seen in Figure 6 and Table 3, generally, increasing the temperature increases the FAME yield, consistent with previous studies referred to [31]. However, it is noteworthy that even at the lower temperature of 40 °C, the study achieved a very high FAME yield of more than 95%. This highlights the effectiveness of the potassium-alumina catalyst in promoting the transesterification reaction at lower temperatures. Achieving such high conversion rates at 40 °C is particularly significant, as it demonstrates the potential for energy savings and reduced operational costs in biodiesel production. Lower reaction temperatures can also minimize the formation of unwanted by-products and reduce the risk of catalyst deactivation.

4. Conclusions

This research aimed to determine the FAME content in biodiesel produced using $K_2O/\gamma\text{-}Al_2O_3$ catalyst and to analyze the effects of reaction temperature, reaction time, and catalyst precursor on the FAME content. The FAME content in the biodiesel ranged from 95.84% to 98.17%, with most samples meeting the SNI 7182:2015 standard of 96.5%, demonstrating the catalyst effectiveness in producing high-quality biodiesel. Even when the synthesis was conducted at a low temperature of 40 °C with 1 hour of reaction time, the potassium-alumina catalyst has proven to be effective in assisting the biodiesel production with high conversion to FAME reaching more than 95% conversion. In this study, the factorial design analysis revealed that the interaction between reaction time and temperature had the most significant impact on yield, followed by temperature and time. This highlights the crucial need to optimize both parameters to maximize FAME content. The catalyst precursor (KI or KNO_3) showed minimal impact on FAME content; the reaction conditions are more influential than the choice of precursor.

Acknowledgement

This research was fully funded by the Center for Research and Community Services of ITB via P3MI Research Grant.

CRediT Author Statement

Author Contributions: Author Contributions: Aghietyas Choirun Az Zahra: Data Analysis, Investigation, Visualization, Writing, Review and Editing; Geraldi Cengko: Formal Analysis, Data Curation, Writing Draft Preparation; Azra Hijran: Validation, Formal Analysis, Writing Draft Preparation; Jenny Rizkiana: Conceptualization, Methodology, Resources, Review and Editing, Supervision. All authors have read and agreed to the published version of the manuscript. All authors have read and agreed to the published version of the manuscript.

References

[1] Sharma, Y.C., Singh, B. (2009). Development of biodiesel: Current scenario. *Renewable and Sustainable Energy Reviews*, 13(6–7), 1646–1651. DOI: 10.1016/J.RSER.2008.08.009.

[2] Szulczyk, K.R, McCarl, B.A. (2010). Market penetration of biodiesel. *Renewable and Sustainable Energy Reviews*, 14(8), 2426–2433. DOI: 10.1016/J.RSER.2010.05.008.

[3] Zahra, A.C.A., Rusyda, I.A., Hizbiyati, A., Giovani, F., Zahara, N., Jiwandaru, B., Gunawan, D., Halim, G.A., Pratiwi, M., Istyami, A.N., Sihombing, A.V.R., Harimawan, A., Sasongko, D., Rizkiana, J. (2021). Novel Approach of Biodiesel Production Waste Utilization to Support Circular Economy in Biodiesel Industry. *IOP Conference Series: Materials Science and Engineering*, 1143(1), 012030. DOI: 10.1088/1757-899x/1143/1/012030.

[4] Wirawan, S.S., Solikhah, M.D., Setiapraja, H., Sugiyono, A. (2024). Biodiesel implementation in Indonesia: Experiences and future perspectives. *Renewable and Sustainable Energy Reviews*, 189, 113911. DOI: 10.1016/J.RSER.2023.113911.

[5] Santosa, S. J. (2008). Palm oil boom in Indonesia: From plantation to downstream products and biodiesel. *Clean - Soil, Air, Water*, 36(5–6), 453–465. DOI: 10.1002/clen.200800039.

[6] Kandasamy, R., Venkatesan, S.K., Uddin, M.I., Ganesan, S. (2020). Anaerobic biovalorization of leather industry solid waste and production of high value-added biomolecules and biofuels. *Biovalorisation of Wastes to Renewable Chemicals and Biofuels*, 3–25. DOI: 10.1016/B978-0-12-817951-2.00001-8

[7] Mahamuni, N.N., Adewuyi, Y.G. (2009). Fourier transform infrared spectroscopy (FTIR) method to monitor soy biodiesel and soybean oil in transesterification reactions, petrodiesel-biodiesel blends, and blend adulteration with soy oil. *Energy and Fuels*, 23(7), 3773–3782. DOI: 10.1021/ef900130m.

[8] Kwon, E.E., Yi, H., Jeon, Y.J. (2013). Mechanistic investigation into water tolerance of non-catalytic biodiesel conversion. *Applied Energy*, 112, 388–392. DOI: 10.1016/J.APENERGY.2013.06.038.

[9] Lam, M.K., Lee, K.T., Mohamed, A.R. (2010). Homogeneous, heterogeneous and enzymatic catalysis for transesterification of high free fatty acid oil (waste cooking oil) to biodiesel: A review. *Biotechnology Advances*, 28(4), 500–518. DOI: 10.1016/J.BIOTECHADV.2010.03.002.

[10] Mandari, V., Devarai, S.K. (2021). Biodiesel Production Using Homogeneous, Heterogeneous, and Enzyme Catalysts via Transesterification and Esterification Reactions: a Critical Review. *BioEnergy Research*, 15(2), 935–961. DOI: 10.1007/S12155-021-10333-W.

[11] Di Serio, M., Tesser, R., Pengmei, L., Santacesaria, E. (2007). Heterogeneous Catalysts for Biodiesel Production. *Energy and Fuels*, 22(1), 207–217. DOI: 10.1021/EF700250G.

[12] Georgogianni, K.G., Katsoulidis, A.K., Pomonis, P.J., Manos, G., Kontominas, M.G. (2009). Transesterification of rapeseed oil for the production of biodiesel using homogeneous and heterogeneous catalysis. *Fuel Processing Technology*, 90(7–8), 1016–1022. DOI: 10.1016/j.fuproc.2009.03.002.

[13] Yang, X.X., Wang, Y.T., Yang, Y.T., Feng, E.Z., Luo, J., Zhang, F., … Bao, G.R. (2018). Catalytic transesterification to biodiesel at room temperature over several solid bases. *Energy Conversion and Management*, 164, 112–121. DOI: 10.1016/J.ENCONMAN.2018.02.085.

[14] Ferella, F., Mazziotti Di Celso, G., De Michelis, I., Stanisci, V., Vegliò, F. (2010). Optimization of the transesterification reaction in biodiesel production. *Fuel*, 89(1), 36–42. DOI: 10.1016/J.FUEL.2009.01.025.

[15] Rashid, U., Anwar, F. (2008). Production of biodiesel through optimized alkaline-catalyzed transesterification of rapeseed oil. *Fuel*, 87(3), 265–273. DOI: 10.1016/J.FUEL.2007.05.003.

[16] Meher, L.C., Vidya Sagar, D., Naik, S.N. (2006). Technical aspects of biodiesel production by transesterification—a review. *Renewable and Sustainable Energy Reviews*, 10(3), 248–268. DOI: 10.1016/J.RSER.2004.09.002.

[17] Sharma, V., Hossain, A.K., Griffiths, G., Duraisamy, G., Thomas, J.J. (2022) Investigation on yield, fuel properties, ageing and low temperature flow of fish oil esters. *Energy Conversion and Management: X*, 14, 100217, DOI: 10.1016/j.ecmx.2022.100217.

[18] Veitía-de-Armas, L., Reynel-Ávila, H.E., Bonilla-Petriciolet, A., Jáuregui-Rincón, J. (2024) Green solvent-based lipid extraction from guava seeds and spent coffee grounds to produce biodiesel: Biomass valorization and esterification/transesterification route, *Industrial Crops and Products*, 214, 118535. DOI: 10.1016/J.INDCROP.2024.118535.

[19] Ngige, G.A., Ovuoraye, P.E., Igwegbe, C.A., Fetahi, E., Okeke, J.A., Yakubu, A.D., Onyechi, P.C. (2023) RSM optimization and yield prediction for biodiesel produced from alkali-catalytic transesterification of pawpaw seed extract: Thermodynamics, kinetics, and Multiple Linear Regression analysis, *Digital Chemical Engineering*, 6, 100066. DOI: 10.1016/J.DCHE.2022.100066.

[20] Prins, R. (2020). On the structure of γ-Al2O3. *Journal of Catalysis*, 392, 336–346. DOI: 10.1016/J.JCAT.2020.10.010.

[21] Xie, W., Li, H. (2006). Alumina-supported potassium iodide as a heterogeneous catalyst for biodiesel production from soybean oil. Journal of *Molecular Catalysis A: Chemical*, 255(1–2), 1–9. DOI: 10.1016/J.MOLCATA.2006.03.061.

[22] Da Costa Evangelista, J.P., Gondim, A.D., Souza, L.Di, Araujo, A.S. (2016). Alumina-supported potassium compounds as heterogeneous catalysts for biodiesel production: A review. *Renewable and Sustainable Energy Reviews*, 59, 887–894. DOI: 10.1016/j.rser.2016.01.061.

[23] Baltrusaitis, J., Schuttlefield, J., Jensen, J.H., Grassian, V.H. (2007). FTIR spectroscopy combined with quantum chemical calculations to investigate adsorbed nitrate on aluminium oxide surfaces in the presence and absence of co-adsorbed water. *Physical Chemistry Chemical Physics*, 9(36), 4970–4980. DOI: 10.1039/b705189a.

[24] Evangelista, J.P.C., Chellappa, T., Coriolano, A.C.F., Fernandes, V.J., Souza, L.D., Araujo, A.S. (2012). Synthesis of alumina impregnated with potassium iodide catalyst for biodiesel production from rice bran oil. *Fuel Processing Technology*, 104, 90–95. DOI: 10.1016/J.FUPROC.2012.04.028.

[25] Zhu, J.H., Wang, Y., Chun, Y., Wang, X.S. (1998). Dispersion of potassium nitrate and the resulting basicity on alumina and zeolite NaY. *Journal of the Chemical Society - Faraday Transactions*, 94(8), 1163–1169. DOI: 10.1039/a708070k.

[26] Singh, D., Yadav, S., Bharadwaj, N., Verma, R. (2020). Low temperature steam gasification to produce hydrogen rich gas from kitchen food waste: Influence of steam flow rate and temperature. *International Journal of Hydrogen Energy*, 45(41), 20843–20850. DOI: 10.1016/J.IJHYDENE.2020.05.168.

[27] Hsieh, L.S., Kumar, U., Wu, J.C.S. (2010). Continuous production of biodiesel in a packed-bed reactor using shell–core structural Ca(C3H7O3)2/CaCO3 catalyst. *Chemical Engineering Journal*, 158(2), 250–256. DOI: 10.1016/J.CEJ.2010.01.025.

[28] Marinković, M., Waisi, H., Blagojević, S., Zarubica, A., Ljupković, R., Krstić, A., & Janković, B. (2022). The effect of process parameters and catalyst support preparation methods on the catalytic efficiency in transesterification of sunflower oil over heterogeneous KI/Al2O3-based catalysts for biodiesel production. *Fuel*, 315, 123246. DOI: 10.1016/J.FUEL.2022.123246.

[29] Wu, W., Zhu, M., Zhang, D. (2017). An experimental and kinetic study of canola oil transesterification catalyzed by mesoporous alumina supported potassium. *Applied Catalysis A: General*, 530, 166–173. DOI: 10.1016/J.APCATA.2016.11.029.

[30] Xiao, Y., Gao, L., Xiao, G., & Lv, J. (2010). Kinetics of the transesterification reaction catalyzed by solid base in a fixed-bed reactor. *Energy and Fuels*, 24(11), 5829–5833. DOI: 10.1021/ef100966t.

[31] Zanjani, N.G., Pirzaman, A.K., Yazdanian, E. (2020). Biodiesel production in the presence of heterogeneous catalyst of alumina: Study of kinetics and thermodynamics. *International Journal of Chemical Kinetics*, 52(7), 472–484. DOI: 10.1002/kin.21363.

[32] Nježić, Z.B., Kostić, M.D., Marić, B.D., Stamenković, O.S., Šimurina, O.D., Krstić, J., Veljković, V.B. (2023) Kinetics and optimization of biodiesel production from rapeseed oil over calcined waste filter cake from sugar beet processing plant, *Fuel*, 334, 126581. DOI: 10.1016/J.FUEL.2022.126581.